

Efficient Origami Construction of Orthogonal Terrains using Cross Section Evolution

Amartya Shankha Biswas, Erik D. Demaine, Jason S. Ku

Abstract: *We introduce a new method of origami construction, using cross section diagrams. Instead of beginning our construction from a 2-dimensional sheet of paper, we consider a 1-dimensional cross section moving forwards in time. We obtain conditions for the validity of a particular cross section evolution sequence, and prove that the resulting folded state is isometric to a flat sheet of paper.*

Subsequently, we use this machinery to design an efficient construction of orthogonal terrains, with arbitrary rational extrusion heights.

1 Introduction

Many algorithms and universality results exist for producing parameterized families of origami structures, but few are provably efficient, i.e. provide constructions from a paper having dimensions within a low constant factor of an optimal construction. At 5OSME, [Demaine et al. 10] presented an efficient construction for folding orthogonal mazes which is computable in polynomial time. Origamizer, presented in [Demaine and Tachi 17] constructs foldings corresponding to general polyhedral surfaces, but does not provide any bound on the efficiency of the constructions. On the other hand, TreeMaker from [Lang 96] produces efficient crease patterns to fold uniaxial bases, but may require exponential time to find an efficient solution.

In this paper, we present an algorithm for efficiently producing an origami folding that corresponds to an input **orthogonal terrain** with arbitrary rational extrusion heights. A folding corresponds to an orthogonal terrain if the folding covers every point on the terrain, but no point on the folding exists above the terrain. This result improves an algorithm, [Benbernou et al. 10] also presented at 5OSME, applicable to a more general class of inputs, providing a universal construction to fold general orthogonal polyhedra, though the construction is less efficient than our construction applied to orthogonal terrains. Our construction approach follows three steps:

1. Decompose the orthogonal terrain into strips, constant along one dimension.
2. Cover the strips efficiently using rectangular strips of paper.
3. Stitch the strips together along matching boundaries.

In order to better communicate the algorithm and the final folded state produced, we also introduce a new **cross section evolution** representation of a folded isometry: a straight line is swept across the crease pattern of a folded surface, and we keep track of how the folding of the line evolves as a cross section of the folded surface. The propagation of the cross section between crease pattern vertices is uniquely determined by the initial orientation of the cross section, so the folded isometry can be constructed by sweeping the line and locally modifying the cross section when crossing crease pattern vertices during propagation. This representation not only simplifies the description of the 3D folded isometries constructed, but also provides a simpler framework to argue that the folded state does not self intersect, by propagating planar cross sections monotonically along a single direction. We then show that our construction's efficiency is within a small constant factor of any folding with optimal efficiency.

2 Cross Section Evolution

We introduce a new method of origami construction, using cross section diagrams. Instead of beginning our construction from a 2-dimensional sheet of paper, we consider a 1-dimensional cross section moving forwards in time through 3D space. A simple example using strip narrowing [Demaine et al. 00] is demonstrated in Figure 4.

2.1 Segments and Cross Sections

Definition 1. A segment s is an oriented line segment with left and right endpoints s_l and s_r . Each segment is also associated with an orientation vector $\hat{\mathbf{o}}_s \equiv \frac{\mathbf{s}_r - \mathbf{s}_l}{\|\mathbf{s}_r - \mathbf{s}_l\|}$. This vector serves to disambiguate the orientation of zero length segments.

Definition 2. A cross section C is defined as an ordered list of line segments $\langle s_1, s_2, \dots, s_n \rangle$, such that for every segment s_i (except the last), the right endpoint of s_i coincides with the left endpoint of s_{i+1} . Each segment s is also associated with a velocity vector $\hat{\mathbf{v}}_s$ of unit magnitude. For a segment $s_i \in C$ we will also denote this velocity as $\hat{\mathbf{v}}_i$.

Invariant 1. All non-joint nodes on a segment s have the same velocity $\hat{\mathbf{v}}_s$.

Invariant 2. The velocity $\hat{\mathbf{v}}_s$ of segment s is orthogonal to its orientation $\hat{\mathbf{o}}_s$.

Definition 3. Given a cross section $C = \langle s_1, s_2, \dots, s_n \rangle$, a node x denotes a point on one of the segments s_i . A joint node is a node that resides on the endpoint of a segment. The distance between two nodes on a cross section is defined as the overall length of cross section between the two nodes.

2.2 Joints

Definition 4. A cross section with n segments is also associated with a list of joints $\langle J_1, \dots, J_{n-1} \rangle$, where J_i corresponds to the right endpoint of s_i (same as left endpoint of s_{i+1}). A particular joint J_i is associated with a left segment s_i , a right segment s_{i+1} , and a velocity J_v .

Definition 5. A joint plane is the plane that coincides with both segments l and r associated with a particular joint J . In case the two segments are coincident (i.e. $\hat{\mathbf{o}}_l = \pm\hat{\mathbf{o}}_r$), we define the joint plane to be orthogonal to $\hat{\mathbf{v}}_l = \hat{\mathbf{v}}_r$.

Definition 6. Consider a joint J associated with segments l , r , and joint plane \mathcal{P} , where $\hat{\mathbf{v}}_l$ and $\hat{\mathbf{v}}_r$ are the velocities of segments l and r . We define $\hat{\mathbf{v}}_l^{\parallel}$ and $\hat{\mathbf{v}}_l^{\perp}$ as components of $\hat{\mathbf{v}}_l$, such that $\hat{\mathbf{v}}_l^{\parallel}$ is the projection of $\hat{\mathbf{v}}_l$ onto \mathcal{P} , and $\hat{\mathbf{v}}_l^{\perp} = \hat{\mathbf{v}}_l - \hat{\mathbf{v}}_l^{\parallel}$ (orthogonal to \mathcal{P}). Similarly, we define $\hat{\mathbf{v}}_r^{\parallel}$ and $\hat{\mathbf{v}}_r^{\perp}$ as the components of $\hat{\mathbf{v}}_r$. By Invariant 2, $\hat{\mathbf{v}}_l^{\parallel}$ and $\hat{\mathbf{v}}_r^{\parallel}$ are orthogonal to $\hat{\mathbf{o}}_l$ and $\hat{\mathbf{o}}_r$ respectively. This uniquely determines the direction of all velocity components.

Henceforth, we will refer to the $\hat{\mathbf{v}}^{\parallel}$ component as the *joint plane velocity*, and the $\hat{\mathbf{v}}^{\perp}$ component as the *joint orthogonal velocity*,

Invariant 3. For a joint J associated with segments l and r , $\hat{\mathbf{v}}_l^{\perp} = \hat{\mathbf{v}}_r^{\perp}$ i.e. the joint orthogonal velocities have to be equal, such that the joint plane moves with a fixed velocity along its normal. As a corollary, $\|\hat{\mathbf{v}}_l^{\parallel}\| = \|\hat{\mathbf{v}}_r^{\parallel}\|$.

2.3 Time Travel

In the process of time travel, all the nodes on a segment s , except the *joint nodes* move with velocity $\hat{\mathbf{v}}_s$ (orthogonal to $\hat{\mathbf{o}}_s$). For example, if we allow a single segment of length X to evolve for time T , it will result in a $X \times T$ strip of paper.

The joint node velocity \mathbf{J}_v may have a component along a corresponding segment s (along $\hat{\mathbf{o}}_s$). As a result, the lengths of segments may change (Figure 2b). This can be visualized as movement of the corresponding joint along one of the segments.

Definition 7. For every segment s in a cross section C , we associate a *left pace* L_s , which indicates the rate at which s shrinks from its left endpoint. Similarly, we define a *right pace* R_s grows from its right endpoint. Note that both these quantities can be negative.

After time T , the length of a segment changes by $T(R_s - L_s)$. The length of a segment is not allowed to become negative. For a segment s_i with left joint J^L and right joint J^R , we obtain the relations

$$\mathbf{J}_v^L - \hat{\mathbf{v}}_{s_i} = L_{s_i} \hat{\mathbf{o}}_{s_i}, \quad \mathbf{J}_v^R - \hat{\mathbf{v}}_{s_i} = R_{s_i} \hat{\mathbf{o}}_{s_i}.$$

Definition 8. A joint J corresponding to segments s and t is valid if and only if the evolution resulting from the velocities $\hat{\mathbf{v}}_l$, $\hat{\mathbf{v}}_r$, and \mathbf{J}_v preserves distances between the non-joint nodes.

Invariant 4. The right pace of s_i is equal to the left pace of s_{i+1} . This is to preserve the overall length of the cross section, and the distance between any two nodes. Furthermore, the left pace of the first segment, and the right pace of the last segment should be zero, i.e., $L_0 = R_n = 0$. This ensures that the total length of the cross section does not change.

The movement of a joint increases the length of one of its associated segments, and decreases the length of the other segment by the same amount (this ensures that the total length is preserved). This puts some constraints on the possible velocities of adjacent segments.

Consider a joint \mathbf{J}_i corresponding to segments $l = s_i$ and $r = s_{i+1}$, at time $t = 0$. Henceforth, we will refer to L_r as L , and R_l as R . Without loss of generality, we assume that $L < 0$. At a later time t , let the new joint position be \mathbf{J}'_i . We define nodes a and b corresponding to \mathbf{J}_i and \mathbf{J}_{i+1} respectively. We also define the initial and final positions of a as \mathbf{a} , and \mathbf{a}' , and similarly for b , we define \mathbf{b} and \mathbf{b}' . Let d be the *separation* between nodes a and b . This setup is shown in Figure 1.

First, note that \mathbf{a}, \mathbf{b} lie on the segment l , and \mathbf{a}', \mathbf{b}' lie on the segment r , which implies that $\mathbf{b} - \mathbf{a} = d\hat{\mathbf{o}}_l$, and $\mathbf{b}' - \mathbf{a}' = d\hat{\mathbf{o}}_r$:

$$\begin{aligned} \mathbf{b}' - \mathbf{a}' &= (\mathbf{b} + t\hat{\mathbf{v}}_r^{\parallel}) - (\mathbf{a} + t\hat{\mathbf{v}}_l^{\parallel}) \\ \implies \mathbf{b}' - \mathbf{a}' &= (\mathbf{b} - \mathbf{a}) + t(\hat{\mathbf{v}}_r^{\parallel} - \hat{\mathbf{v}}_l^{\parallel}) \\ \implies d\hat{\mathbf{o}}_r &= d\hat{\mathbf{o}}_l + t(\hat{\mathbf{v}}_r^{\parallel} - \hat{\mathbf{v}}_l^{\parallel}) \\ \implies \hat{\mathbf{v}}_r^{\parallel} - \hat{\mathbf{v}}_l^{\parallel} &= \frac{d}{t}(\hat{\mathbf{o}}_r - \hat{\mathbf{o}}_l) = -R(\hat{\mathbf{o}}_r - \hat{\mathbf{o}}_l) \\ &= -L(\hat{\mathbf{o}}_r - \hat{\mathbf{o}}_l). \end{aligned}$$

This is only possible if $\hat{\mathbf{o}}_l \times \hat{\mathbf{o}}_r$ is oriented opposite to $\hat{\mathbf{v}}_l^{\parallel} \times \hat{\mathbf{v}}_r^{\parallel}$.

Invariant 5. Given two adjacent segments l and r in a cross section C , the vector $\hat{\mathbf{o}}_l \times \hat{\mathbf{o}}_r$ must be oriented opposite to $\hat{\mathbf{v}}_l^{\parallel} \times \hat{\mathbf{v}}_r^{\parallel}$.

If the angle between the segments (between $\hat{\mathbf{o}}_l$ and $\hat{\mathbf{o}}_r$) is θ , the magnitude of $\hat{\mathbf{o}}_r - \hat{\mathbf{o}}_l$ is $\sqrt{2 - 2\cos(\theta)}$, and $\|\hat{\mathbf{v}}_r^{\parallel} - \hat{\mathbf{v}}_l^{\parallel}\| = v \cdot \sqrt{2 - 2\cos(\pi - \theta)}$. Here, v is magnitude of the plane velocity (projection onto the joint plane \mathcal{P}) of \mathbf{J}_i . Given $\omega = \theta/2$, we get:

$$-L = -R = \frac{d}{t} = \hat{\mathbf{v}}_l - \hat{\mathbf{o}}_l \frac{\|\hat{\mathbf{v}}_r^{\parallel} - \hat{\mathbf{v}}_l^{\parallel}\|}{\|\hat{\mathbf{o}}_r - \hat{\mathbf{o}}_l\|} = v \cdot \frac{\sqrt{\sin^2(\pi/2 - \theta/2)}}{\sqrt{\sin^2 \theta/2}} = v \cdot \cot(\omega).$$

Invariant 6. The velocity of a joint J associated with segments l and r , is a constant vector $\mathbf{J}_v = \hat{\mathbf{v}}_l - \|\hat{\mathbf{v}}_l^{\parallel}\| \hat{\mathbf{o}}_l \cdot \cot(\theta/2)$, where θ is the angle between $\hat{\mathbf{o}}_l$ and $\hat{\mathbf{o}}_r$.

2.4 Cross Section Interval Folding

Definition 9. We consider a cross section composed of segments $\langle s_1, s_2, \dots, s_n \rangle$ with total length X (i.e., $\sum |s_i| = X$). If we allow this cross section to evolve for time T , we obtain a new cross section $\langle r_1, r_2, \dots, r_n \rangle$. The evolution forms a cross section interval \mathcal{C} of length T . The initial cross section is denoted as $\mathcal{C}_I = \langle s_1, s_2, \dots, s_n \rangle$, and the final cross section is denoted as $\mathcal{C}_F = \langle r_1, r_2, \dots, r_n \rangle$.

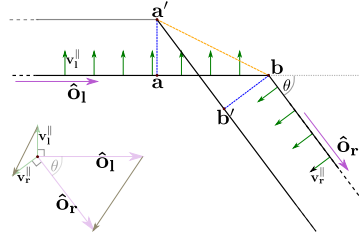


Figure 1: A joint with segments l and r . The trajectory of the joint is shown in orange. The trajectories of a and b are shown in blue. The green arrows indicate \mathbf{v}^{\parallel} .

In this section, we focus on a single cross section interval \mathcal{C} with segments $\langle s_1, s_2, \dots, s_n \rangle$ evolving over time T . First consider the surface traced out by an individual segment s_i . Since the endpoints of s_i move in a straight line, each segment traces a trapezoid. We define the *height* of a trapezoid to be the distance between its parallel sides.

Lemma 1. *The surface traced out by a segment s in time T is a trapezoid Z_s of height T (Figure 2a). Specifically, if L, R are the initial left and right endpoints of s , and L', R' are the final endpoints, $Z_s = LL'R'R$ is the corresponding trapezoid (Figure 2a).*

Proof. By Invariant 6, we know that the joint trajectories are straight lines, which form the non-parallel sides. Since the non-joint nodes on a segment all have the same velocity, the initial and final segment positions form the parallel sides. \square

Lemma 2. *Consider a joint J with segments l and r , which has zero orthogonal joint velocity (i.e., $\mathbf{v}_l^\perp = \mathbf{v}_r^\perp = \mathbf{0}$). The gluing of trapezoids Z_l and Z_r along the joint trajectory \mathcal{T}_J is isometric to a larger trapezoid.*

Proof. We consider the evolution of joint J for time T (Figure 2b). First consider a coordinate system with $(\hat{\mathbf{v}}_l, \hat{\mathbf{o}}_l)$ as the basis. Since, $\hat{\mathbf{v}}_l = \mathbf{v}_l^\perp$, from Invariant 6, we know that $-R_l = \|\mathbf{v}_l^\perp\| \cot(\omega) = \cot(\omega)$. So, $\mathbf{J}_v = \hat{\mathbf{v}}_l - \hat{\mathbf{o}}_l \cot(\omega)$. Therefore,

$$\cot(\angle LJJ') = \frac{-TR_l}{\|T\hat{\mathbf{v}}_l\|} = \cot(\omega) \implies \angle LJJ' = \omega.$$

Similarly, we consider a coordinate system with $(\hat{\mathbf{v}}_r, \hat{\mathbf{o}}_r)$ as the basis, with $-L_r = \|\mathbf{v}_r^\perp\| \cot(\omega) = \cot(\omega)$. Since $\mathbf{J}_v = \hat{\mathbf{v}}_r - \hat{\mathbf{o}}_r \cot(\omega)$, we get

$$\cot(\angle RJJ') = \frac{TL_r}{\|T\hat{\mathbf{v}}_r\|} = -\cot(\omega) \implies \angle RJJ' = \pi - \omega.$$

This implies that $\cot(\angle RJJ') + \cot(\angle LJJ') = \pi$. So, the gluing of Z_l and Z_r along the joint trajectory JJ' is isometric to a larger trapezoid. \square

Lemma 3. *Consider a joint J with segments l and r with non-zero orthogonal velocity; see Figure 3. The gluing of trapezoids Z_l and Z_r along the joint trajectory \mathcal{T}_J is isometric to a larger trapezoid.*

Proof. As before, let LJR and $L'J'R'$ represent the initial and final positions of the segments respectively. We also construct the projection of $L'J'R'$ to the joint plane \mathcal{P} as $L''J''R''$. The evolution of the projection is analogous to the setting in Lemma 2. Therefore, $\angle LJJ'' = \omega = \theta/2$ and $\angle RJJ'' = \pi - \omega$.

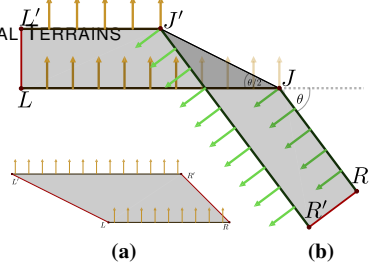


Figure 2: Trapezoid formed by evolving line segment (a), and the gluing of two adjacent trapezoids (b).

Consider the positive z -axis along the joint orthogonal velocity (i.e., normal to the joint plane \mathcal{P}). We define the orthogonal displacement vector as $\vec{JJ}' = z\hat{\mathbf{k}}$. Let the positive x -axis be along JJ'' . So, the unit vector along \vec{JJ}' is $\frac{1}{\sqrt{1+z^2}}(1, 0, z)$.

Since $\angle J''JR = \omega$, the unit vector along \vec{JR} is $(\cos \omega, \sin \omega, 0)$. So, we compute $\cos \angle RJJ' = \cos \omega / \sqrt{1+z^2}$. Similarly, since $\angle J''JL = \pi - \omega$, the unit vector along \vec{JL} is $(-\cos \omega, \sin \omega, 0)$, which implies that $\cos \angle LJJ' = -\cos \omega / \sqrt{1+z^2}$. Finally, since both $\angle LJJ'$ and $\angle RJJ'$ are less than π , and $\cos(\angle LJJ') = -\cos(\angle RJJ')$, we conclude that $\angle LJJ' + \angle RJJ' = \pi$. Since $LJJ'L'$ and $RJJ'R'$ are both trapezoids, this implies that the resulting gluing along JJ' is isometric to a larger trapezoid. \square

Definition 10. Consider a cross section interval \mathcal{C} formed from a cross section C evolving over time T . By Lemma 1, the segments $\langle s_1, s_2, \dots, s_n \rangle$ form trapezoids $\langle Z_1, Z_2, \dots, Z_n \rangle$ each of height T , where Z_i represents the i^{th} trapezoid in folded space. The folded surface \mathcal{F}_C^T corresponding to \mathcal{C} is formed by successively gluing the trapezoids Z_i to Z_{i+1} along the trajectory of joint \mathbf{J}_i (for $1 \leq i < n$) to form a connected shape.

Definition 11. Given a cross section interval \mathcal{C} with folding \mathcal{F}_C^T , the initial-boundary of a folding \mathcal{F}_C^T is defined as the union of the initial cross section segments in \mathcal{C}_I , where the right endpoint of the i th segment is attached to the left endpoint of the $(i+1)$ st segment. Similarly, the final-boundary of \mathcal{F}_C^T is defined as the union of the final segments in \mathcal{C}_F .

Theorem 4. Consider a cross section interval \mathcal{C} formed from a cross section C evolving over time T to form a folding \mathcal{F}_C^T . Further assume that the total length of cross section C is X units. Then, \mathcal{F}_C^T is isometric to a $X \times T$ strip of paper.

Proof. By repeated use of Lemma 3, we know that \mathcal{F}_C^T is isometric to a trapezoid. Let L, L' be the initial and final positions of the left (non-parallel) edge of the trapezoid, and let R, R' be the initial and final positions of the right edge of the trapezoid. Say that C comprises of segments $\langle s_1, s_2, \dots, s_n \rangle$. From Invariant 4, we know that the left pace of s_0 is zero. So, the line LL' follows the trajectory of $\hat{\mathbf{v}}_0$, which is orthogonal to the segment s_0 . In other words, the left edge of the trapezoid has length T , and is orthogonal to the parallel edges. Similarly, because the right pace of s_n is zero, the right edge of the trapezoid is also orthogonal. Therefore, \mathcal{F}_C^T is isometric to a right angled trapezoid (i.e., a strip) of length X and width T . \square

Remark 1. The trajectory of a joint forms a crease in the folded state.

2.5 Multiple Cross Sections

Definition 12. Given two cross section intervals \mathcal{C} and \mathcal{D} , such that \mathcal{C}_F and \mathcal{D}_I are equivalent, we say that \mathcal{D} is next-compatible with \mathcal{C} and \mathcal{C} is previous-compatible with \mathcal{D} . Two cross sections $C = \langle s_1, s_2, \dots, s_n \rangle$ and $D = \langle r_1, r_2, \dots, r_m \rangle$ are equivalent if and only if C and D correspond to the same sequence of segments after the deletion of all zero length segments.

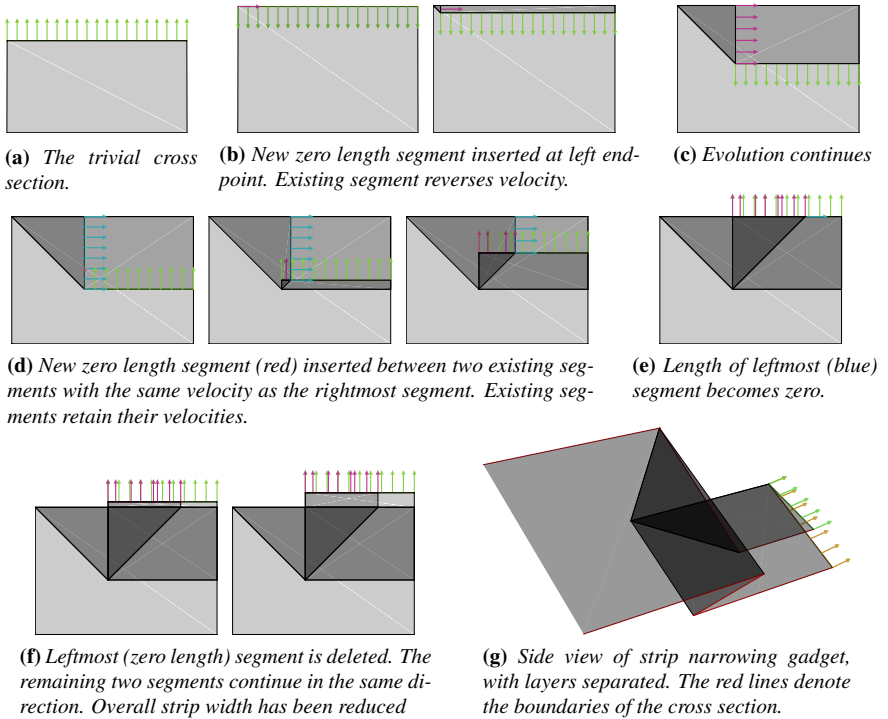


Figure 4: Cross section evolution of a strip narrowing gadget [Demaine et al. 00].

Definition 13. A cross section sequence is a sequence is an ordered list of cross section intervals $\langle \mathcal{C}_1, \mathcal{C}_2, \dots, \mathcal{C}_n \rangle$, such that \mathcal{C}_i is next-compatible with \mathcal{C}_{i-1} for all $i \in [2, n]$. This is equivalent to stating that \mathcal{C}_i is previous-compatible with \mathcal{C}_{i+1} for all $i \in [1, n - 1]$. Note that we do not care about the velocities of the segments.

We will represent our full construction as a valid cross section sequence. Given a cross section sequence $\langle \mathcal{C}_1, \mathcal{C}_2, \dots, \mathcal{C}_n \rangle$, the transition from \mathcal{C}_i to \mathcal{C}_{i+1} corresponds to the deletion of one or more length zero segments from \mathcal{C}_i , and the addition of one or more zero length segments to obtain \mathcal{C}_{i+1} . Figure 4 shows a simple example.

Definition 14. Given a cross section sequence $\langle \mathcal{C}_1, \mathcal{C}_2, \dots, \mathcal{C}_n \rangle$, We obtain \mathcal{F}_i^T as the folding of cross section \mathcal{C}_i .

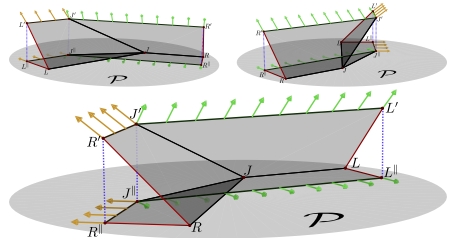


Figure 3: Evolution of a joint with non-zero orthogonal velocity from LJR to $L'J'R'$. The blue dotted lines are the projection of the final state to the joint plane \mathcal{P} .

For each $i \leq n - 1$, we attach \mathcal{F}_i^T to \mathcal{F}_{i+1}^T by gluing the final cross section of \mathcal{C}_i to the initial cross section of \mathcal{C}_{i+1} . This results in the final folding of the cross section sequence.

Proposition 1. *In addition to the creases formed along the trajectory of joints (Remark 1), creases are also created when a segment changes velocity. For instance, consider two adjacent cross sections \mathcal{C} and \mathcal{D} , with corresponding segments $s_C \in \mathcal{C}_F$ and $s_D \in \mathcal{D}_I$, where s_C and s_D are identical except for their velocity direction. Then, the segment s_C (same as s_D) forms a crease in the folded state.*

2.5.1 Evolution Corresponds to Flat Paper

In this section we will demonstrate that the folding formed by cross section evolution is realizable from a sheet of flat paper. We note here that our construction may still result in self intersections.

We consider a cross section sequence $\langle \mathcal{C}_1, \mathcal{C}_2, \dots, \mathcal{C}_n \rangle$, where each cross section interval \mathcal{C}_i has evolution time T_i . We then use Theorem 13 to attach the sequence of $X \times T_i$ strips, to form a complete $X \times T$ sheet of paper, where $T = \sum T_i$.

Theorem 5. *Consider a cross section sequence $\mathcal{C} = \langle \mathcal{C}_1, \mathcal{C}_2, \dots, \mathcal{C}_m \rangle$ where each cross section interval \mathcal{C}_i evolves over time T_i to form a folding \mathcal{F}_i such that Invariants 1-6 hold for all segments and joints in each of the cross sections involved. Then, the folding $\mathcal{F}_{\mathcal{C}}$ obtained by successively gluing the final boundary of \mathcal{F}_i to the initial boundary of \mathcal{F}_{i+1} (for each $1 \leq i < m$), is isometric to a $X \times T$ strip of paper, where $T = \sum T_i$.*

Proof. From Theorem 4, we know that each \mathcal{F}_i is isometric to a strip Z_i of size $X \times T_i$. Further, the initial and final cross sections of \mathcal{C}_i form the parallel sides of Z_i (of length X). The gluing of n strips of size $X \times T_i$ forms a strip of size $X \times T$. So, the final folding is isometric to a sheet of paper with size $X \times T$. \square

3 Orthogonal Terrains

In this section, we outline a construction of orthogonal terrains with arbitrary rational extrusion heights. In our construction, the cross section at will always be on the $x - z$ plane. To simplify the presentation, we will consider an uniform $X - Y$ grid, with arbitrary rational extrusion heights corresponding to every grid square (Figure 5).

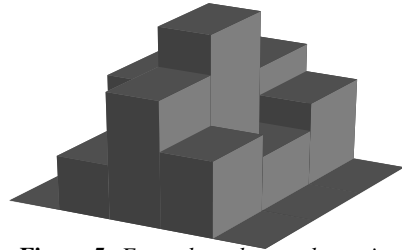


Figure 5: Example orthogonal terrain.

Definition 15. *An $n \times m$ rational grid extrusion is a 3-dimensional structure, whose projection onto the $x - y$ plane forms an unit grid of size $n \times m$. The 3-dimensional structure is formed as the union of $n \times m$ boxes, each with an unit base such that the height of the $(i, j)^{th}$ box is $E_{i,j}$ where $E_{i,j}$ is a rational number.*

We consider each “column” of a given grid extrusion separately as an individual *column extrusion* (Figure 6). We will construct each of the n columns independently (Figure 8), and attach them together with *column connectors* (Figure 12).

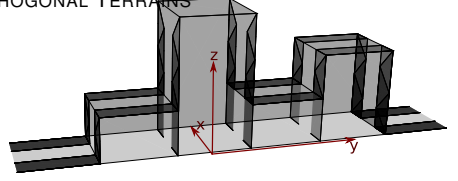


Figure 6: Column extrusion with heights $\{0, 1, 3, 1, 2, 0\}$.

We begin by choosing an $2\epsilon = 1/K$ where K is a positive integer. This is chosen such that $E_{i,j}$ is an integral multiple of 2ϵ for all i, j .

3.1 Construction of Column Extrusion by Level Shifting

First, we consider a single column (Figure 6) of the orthogonal terrain $\{E_{i,1}, E_{i,2}, \dots, E_{i,n}\}$. We denote the column extrusion heights as $\{H_1, H_2, \dots, H_n\}$, where $H_j = E_{i,j}$. Consider the decomposition of T into the following time intervals:

$$T = 1 + D_1 + 1 + D_2 + 1 + D_3 + \dots + 1 + D_{m-1} + 1. \quad (1)$$

Here, the time corresponding to the i th 1 is realized as the surface at height H_i , and the time corresponding to $D_i = |H_i - H_{i+1}|$ is the transition between H_i and H_{i+1} .

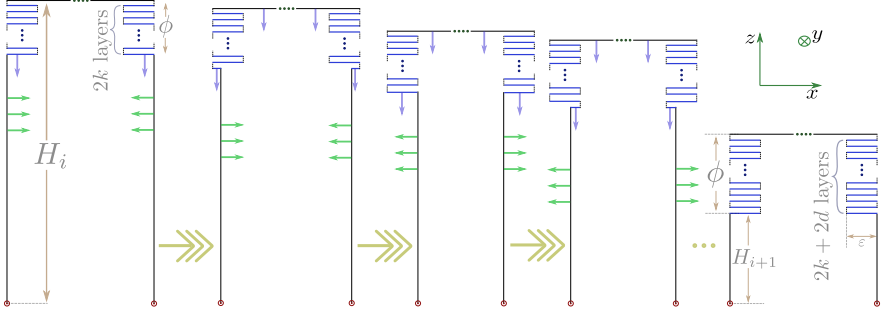


Figure 7: Cross section change from level i to $i+1$. The accordion segments are separated for illustration. In reality, the accordion is folded flat. Zero distances are marked by ϕ . The velocities of horizontal and vertical segments are shown by purple and green arrows respectively.

To construct the column, we will present a cross section sequence. First we describe a *down-shift* gadget. That is, consider i , such that $H_{i+1} = H_i - 2\epsilon \cdot d < H_i$. Figure 7 shows the cross section evolution. This cross section comprises of a two vertical lines separated by a top horizontal line. The vertical lines are connected to the top segment with a sequence of $2k$ horizontal segments that *accordion* back and forth. During each 1-interval, all segments move along the positive y direction (Figure 8a), to create the i th level. Subsequently, during the level shift, all segments move in the $x-z$ plane (Figure 8b, 8c).

Property 1. *The number of accordion folds during horizontal evolution (along the y axis) must be even.*

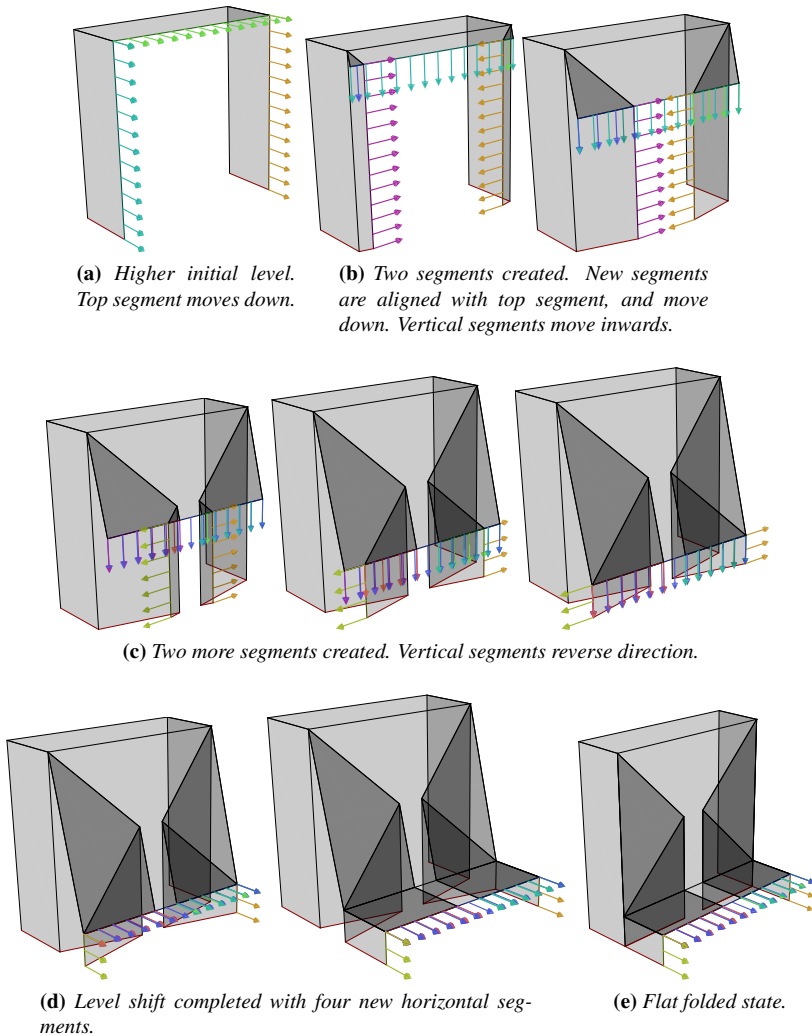


Figure 8: Level shifting gadget. The separation along the Y direction illustrates the layering. The red line denotes the boundary of the cross section.

The top segment moves downwards in intervals of 2ϵ . During this process, the horizontal segments move downwards continuously (Figure 8b, 8c). For the first ϵ time interval, a new horizontal downwards moving accordion segment of length zero is created at both accordions, and the vertical segments move towards each other along the x -axis (Figure 8b). For the next ϵ time interval, similar (oppositely oriented) accordion segments are created at the lowest position. This time, the vertical segments move outwards (Figure 8c), until they reach their original position

(Figure 8d). Overall, two sets of accordion segments on either side are added, and the height of the top segment decreases by 2ϵ .

In the case that $H_{i+1} = H_i + 2\epsilon \cdot d$, the level up-shift is simply the down-shift evolution in reverse (Figure 12). This transition is only possible if the initial number of accordion segments in the H_i cross section is at least $2d$. Specifically, assuming that the minimum height is zero, we have the following lemma.

Lemma 6. *If the number of accordion segments at level H_i is l_i , then the number of accordion segments after transitioning to level H_{i+1} is $l_{i+1} = l_i - (H_{i+1} - H_i)/\epsilon$. Specifically, if the number of layers at level 0 is l , then the number of layers at level $\max\{H_i\}$ is $l - \max\{H_i\}/\epsilon$.*

Corollary 7. *Since the number of accordion segments can never be negative, the minimum number of layers at level zero is $L = \max\{H_i\}/\epsilon$. This also ensures that every other level shift is also possible.*

Corollary 8. *The length of the cross section at a zero level is at least $1 + 2 \cdot L \cdot \epsilon$. So, the minimum possible length of the cross section under our construction is $1 + 2 \cdot \max\{H_i\}$.*

This provides the minimum width of any strip required to construct a column extrusion. Also the minimum required strip length is given by

$$T = 1 + D_1 + 1 + D_2 + 1 + D_3 + \cdots + 1 + D_{m-1} + 1 = m + \sum_{i=1}^{m-1} |H_{i+1} - H_i|.$$

Theorem 9. *A given column extrusion with heights $\{H_1, H_2, \dots, H_n\}$, can be constructed from a strip of paper with size $X \times T$, where*

$$X \geq 1 + 2 \cdot \max\{H_i\}, \quad T \geq \left(m + \sum_{i=1}^{m-1} |H_{i+1} - H_i| \right).$$

3.2 Multiple Column Extrusions form a Grid Extrusion

Now, we consider multiple column extrusions evolving in parallel. Henceforth, we will refer to the evolution of column cross sections along the y -axis (the “1”s in Equation 1) as *horizontal evolution*. Meanwhile, a *vertical transition* will refer to level shifting evolution in the $x-z$ plane. Let $\mathcal{C}^{(i)}$ be a valid cross section evolution corresponding to the i th column in the grid extrusion (as defined in Section 3.1). As before, for simplicity, we will assume that the minimum height in each column is zero (*i.e.* $\min_j \{E_{i,j}\} = 0$).

We consider the parallel evolution of each column extrusion $\mathcal{C}^{(i)}$.

- During the horizontal evolution of row j , each $\mathcal{C}^{(i)}$ evolves along the positive y direction for time 1 at height $E_{i,j}$.
- During the vertical transition from row j to $j+1$, each $\mathcal{C}^{(i)}$ evolves for time $D_{ij} = |E_{i,j+1} - E_{i,j}|$.

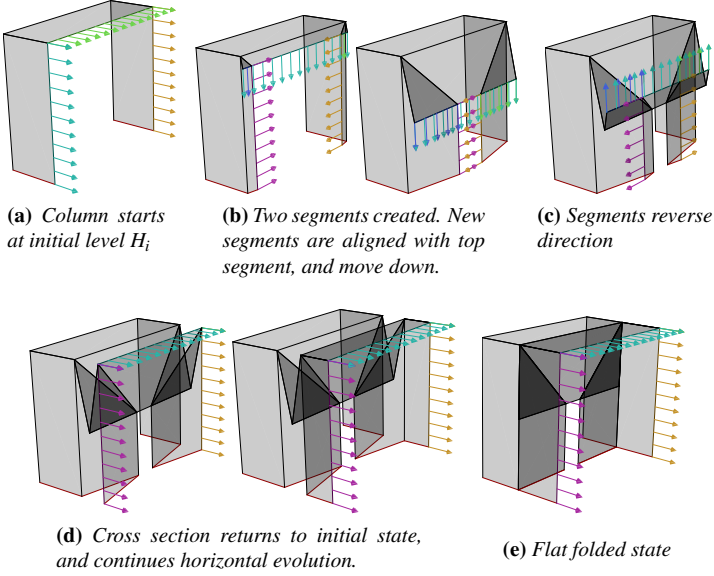


Figure 9: Up-down gadget. The separation along the Y direction illustrates the layering. The red line denotes the boundary of the cross section.

Note that the vertical transition times are different for each $\mathcal{C}^{(i)}$. Since we want to glue the sequence of $\{\mathcal{C}^{(i)}\}$ s, our constructions must have equal transition times.

Definition 16. We define the common transition time from row j to row $j+1$ as

$$D_j = \max_j \{D_{ij}\} = \max_j \{|E_{i,j+1} - E_{i,j}|\}.$$

So, the slowest column dictates the transition time, and the faster columns have to *stall* for additional time. To achieve this, we define an *up-down* gadget, which is very similar to our original level shifting gadget. This up-down gadget (Figure 9) evolves for 2ε time, but the height of the corresponding column remains unchanged. This gadget starts at a height H_i , and for the first ε time interval (Figure 9b), evolves exactly the same way as the down-shift gadget (Figure 8b). For the second ε time interval, the cross section evolves in reverse (Figure 9c), back to its original state at height H_i (Figure 9d).

So, the vertical transition of $\mathcal{C}^{(i)}$ needs to use a total of $(D_j - D_{i,j}) / (2\varepsilon)$ up-down gadgets (each gadget *stalls* for 2ε time). We obtain the following proposition, as a consequence of Theorem 9.

Proposition 2. By Theorem 9, the extrusion for column i is constructed from a paper strip with size

$$\left(1 + 2 \cdot \max_j \{E_{ij}\}\right) \times \left(m + \sum_{j=1}^{m-1} D_j\right).$$

3.3 Gluing Column Extrusions together with Strip Connectors

Now that all the column extrusions $\{\mathcal{E}^{(i)}\}$ have the same evolution time, we would like to glue them together into a continuous strip of paper. In order to achieve this, we consider the time-axis boundaries of $\mathcal{E}^{(i)}$ (red line in Figure 8, 9). First, note that the boundaries always lie on the same plane, corresponding to the zero level. We will constrain this to be on the plane $z = 0$. Now, let us consider the motion of the boundary on this plane.

- During the horizontal evolution of any row j , both boundaries move along the positive y -axis with unit velocity (Figure 8a, 8d, 8e, 9a, 9d, 9e).
- During the vertical transition from row j to $j + 1$, both boundaries move back and forth along the x -axis with unit velocity. (Figure 8b, 8c, 9b, 9c). We can divide the vertical transition into $k = D_j/(2\epsilon)$ intervals of length 2ϵ . Each of these interval segments is either a up-shift, a down-shift, or a up-down gadget.
 - In the first half of each interval (ϵ time), the left and right boundaries move towards each other; i.e., the left boundary moves along the positive x -axis, and the right boundary moves along the negative x -axis for a distance of ϵ .
 - In the second half of each interval, the left and right reverse velocities, and return to their original positions.
 - After D_j time, the boundaries return to their original positions, and resume their movement in the positive y direction.

We will attempt to construct a cross section sequence whose left and right boundaries line up with the adjacent column extrusion boundaries shown in Figure 10. Notice that the distance between *corresponding points* on the boundaries varies between 0 and 2ϵ . So, the connector strip must have width at least 2ϵ .

We outline a construction of a 2ϵ width strip, as shown in Figure 11. During horizontal evolution, the cross section comprises of two vertical segments, each of length ϵ , which move along the same trajectory in the positive y -direction (during horizontal evolution Figure 12a, 12k). Now, consider a transition of length D_j divided into intervals of length 2ϵ , each of which evolves according to Figure 11.

- The vertical segments move outwards with unit velocity to match the outward moving boundaries of the adjacent strips. An upwards moving horizontal segment of length zero is created between the two existing segments (Figure 12b).
- After time ϵ , the length of the vertical segments become zero, and the horizontal segment spans the 2ϵ gap between the column boundaries (Figure 12c). Notice that that the boundary of the connector maintains its z coordinate (Figure 11).

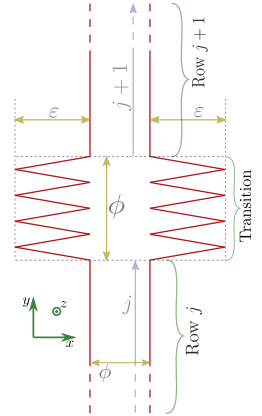


Figure 10: Boundaries of adjacent column extrusions ($D_j = 8\epsilon$). ϕ denotes a zero distance.

- Then the connector segments reverse velocities, and retrace their path for ε time (Figure 12d), until the vertical segments become length ε , and the horizontal segment disappears (Figure 12e).
- The entire process repeats $D_j/(2\varepsilon)$ times (Figure 12f, 12g, 12h).

The completed connector gadget is shown in Figure 12i, 12j. We show the *connector gadget* attached to an *up-shift gadget* in Figure 12h, 12k.

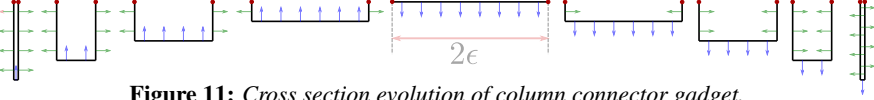


Figure 11: Cross section evolution of column connector gadget.

3.4 Size of Construction

We define $M_i = \max_j \{E_{ij}\}$. From Proposition 2, we know that each column extrusion strip $\mathcal{C}^{(i)}$ has width $(1 + 2 \cdot \max_j \{E_{ij}\}) = 1 + 2 \cdot M_i$. We can ignore the left, and right vertical strips for the leftmost, and rightmost columns. So, the leftmost and rightmost columns use strips of width $(1 + M_0)$ and $(1 + M_n)$ respectively.

Additionally, we have $n - 1$ strip connectors, each of width 2ε . So, the total width of the orthogonal terrain construction is

$$X = 2(n - 1) \cdot \varepsilon + n + 2 \cdot \sum_{i=1}^n M_i - M_0 - M_n.$$

Our construction is also valid for any $\varepsilon' = \varepsilon/(2k)$, where k is an integer. In other words, we can make ε arbitrarily small.

Theorem 10. *Using the time evolution (y dimension) from Proposition 2, we conclude that a grid extrusion can be folded from a strip of size $X \times T$, where*

$$X = n + 2 \cdot \sum_{i=1}^n M_i - M_0 - M_n + o(1), \quad T = m + \sum_{j=1}^{m-1} D_j.$$

3.5 Optimality

Consider a $n \times n$ orthogonal terrain where the highest points along x -axis are $M = \max_j E_{ij}$, and the maximum deltas along the y -axis are $D_j = \max_i \|E_{i,j} - E_{i,j+1}\| = M$. Now, we consider a sort of worst case orthogonal terrain defined as follows:

$$E_{ij} = \begin{cases} M & \text{if } (i + j) \text{ is even,} \\ 0 & \text{if } (i + j) \text{ is odd.} \end{cases}$$

This forms a checkerboard alternating between the minimum and maximum heights. We assume that the top faces of the terrain form axis aligned squares in the unfolded state, The longest line formed along either axis is the total length of the top surfaces plus the sum of the height changes across the axis, which gives

$$L = n + \sum_{i=1}^n M = n + (n - 1) \cdot M.$$

EFFICIENT ORIGAMI CONSTRUCTION OF ORTHOGONAL TERRAINS

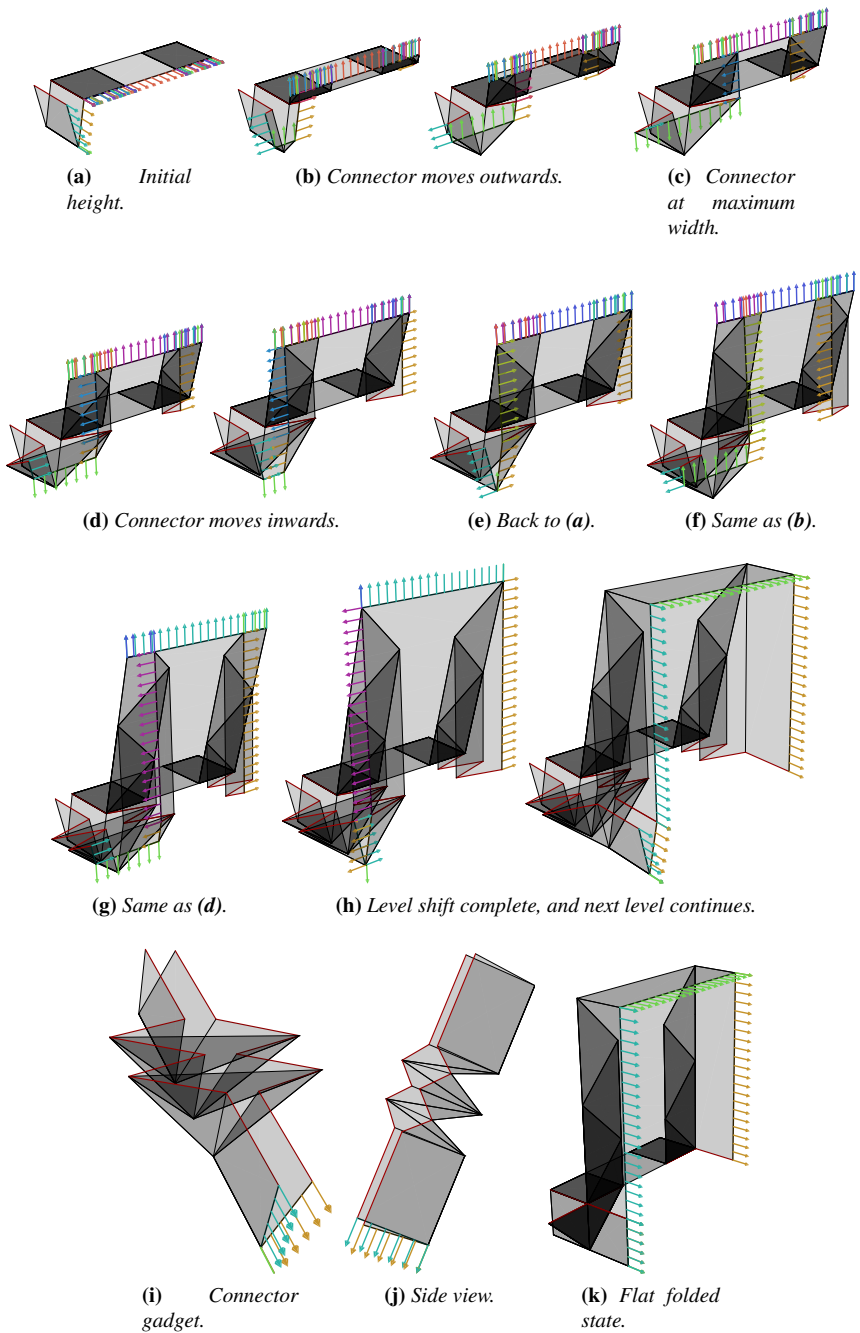


Figure 12: Column gadget attached to a single column connector gadget. The red line demarcates the interface between the two gadgets.

We conclude that the minimum required size of the folding is $L \times L$.

From Theorem 10, we know that the terrain can be folded from a $X \times Y$ strip of paper, where $X = n + 2(n - 1) \cdot M + o(1)$ and $Y = n + (n - 1) \cdot M$. Since $Y = L$, and $X < 2L$ (assuming an appropriately small value of ϵ), our construction results in a folding is within a factor two of the optimal paper usage, under the aforementioned assumption.

This paper provides a universal construction to fold orthogonal terrains that is optimally efficient over its domain, improving upon previous constructions that were less efficient but applicable to a more general class of target shapes, i.e., orthogonal polyhedra. Some natural questions arise. Can one improve the efficiency of the construction for a more restricted set of terrains? For example, our lower bound is achieved by a maximum height-difference checkerboard; perhaps one can improve folding efficiency for terrains that are more slowly varying. Our construction only covers the terrain from above, allowing the folding to exist anywhere in the space below the terrain. This allocation is necessary when points of the terrain have more than 2π material at a point. What is the minimum area of paper that can exist away from the target terrain over all possible foldings?

Acknowledgements: We thank Martin Demaine, Herng Yi Cheng, Aviv Ovadya, and Tomohiro Tachi for helpful discussions about this family of problems at 5OSME.

References

- [Benbernou et al. 10] Nadia M. Benbernou, Erik D. Demaine, Martin L. Demaine, and Aviv Ovadya. “Universal Hinge Patterns to Fold Orthogonal Shapes.” In *Origami⁵: Proceedings of the 5th International Conference on Origami in Science, Mathematics and Education (OSME 2010)*, pp. 405–420. Singapore: A K Peters, 2010.
- [Demaine and Tachi 17] Erik D. Demaine and Tomohiro Tachi. “Origamizer: A Practical Algorithm for Folding Any Polyhedron.” In *Proceedings of the 33rd International Symposium on Computational Geometry (SoCG 2017)*, pp. 34:1–34:15. Brisbane, Australia, 2017.
- [Demaine et al. 00] Erik D. Demaine, Martin L. Demaine, and Joseph S. B. Mitchell. “Folding flat silhouettes and wrapping polyhedral packages: New results in computational origami.” *Computational Geometry: Theory and Applications* 16:1 (2000), 3–21.
- [Demaine et al. 10] Erik D. Demaine, Martin L. Demaine, and Jason Ku. “Folding Any Orthogonal Maze.” In *Origami⁵: Proceedings of the 5th International Conference on Origami in Science, Mathematics and Education (OSME 2010)*, pp. 449–454. Singapore: A K Peters, 2010.
- [Lang 96] Robert J. Lang. “A computational algorithm for origami design.” In *Proc. 12th Symp. Computational Geometry*, pp. 98–105. Philadelphia, PA, 1996.